Optics Letters

Three-wave mixing of ordinary and backward electromagnetic waves: extraordinary transients in the nonlinear reflectivity and parametric amplification

Vitaly V. Slabko,[1] Alexander K. Popov,[2,*] Viktor A. Tkachenko,[1] and Sergey A. Myslivets[1,3]

[1]Siberian Federal University, 79 Svobodny Av., Krasnoyarsk 660041, Russian Federation
[2]Birck Nanotechnology Center, Purdue University, 1205 W State St., West Lafayette, Indiana 47907, USA
[3]L. V. Kirensky Institute of Physics, Siberian Branch of the Russian Academy of Sciences, Krasnoyarsk 660036, Russian Federation
*Corresponding author: popov@purdue.edu

Received 30 June 2016; revised 3 August 2016; accepted 4 August 2016; posted 4 August 2016 (Doc. ID 269399); published 23 August 2016

Three-wave mixing of ordinary and backward electromagnetic waves in a pulsed regime is investigated in the metamaterials that enable the coexistence and phase-matching of such waves. It is shown that the opposite direction of phase velocity and energy flux in backward waves gives rise to extraordinary transient processes due to greatly enhanced optical parametric amplification and frequency up- and down-shifting nonlinear reflectivity. The differences are illustrated through comparison with the counterparts in ordinary, co-propagating settings.

OCIS codes: (190.4223) Nonlinear wave mixing; (190.4410) Nonlinear optics, parametric processes; (190.5530) Pulse propagation and temporal solitons; (160.3918) Metamaterials.

http://dx.doi.org/10.1364/OL.41.003976

Advances in nanotechnology have made possible the engineering of the metamaterials (MMs) that support optical backward electromagnetic waves (BEMWs). Counterintuitively, energy flux and phase velocity are *contra-directed* in BEMWs. Such waves may exist only in a certain frequency range dependent on particular MMs whereas only ordinary EMWs propagate outside the backward wave (BW) frequency band. The emergence of optical BEMWs gives rise to revolutionary breakthroughs in linear photonics and its applications, such as sub-wavelength resolution and cloaking, which are not possible with ordinary optical EMWs [1]. This justifies studies on nonlinear-optical (NLO) techniques for excitation and control of BEMWs. Exciting possibilities were predicted in nonlinear photonics, such as huge enhancements in wave mixing through implementation of a BEMW as one of the coupled waves (see [1–3] and references therein). Extraordinary enhancement in coherent energy transfer from the ordinary pump waves to contra-propagating BEMWs at different frequencies can be employed for compensating losses inherent to BEMWs in plasmonic MMs and to broaden a spectrum of achievable BEMWs and their use in photonics. Among them are ultracompact optical parametric amplifiers (OPAs) and cavity-free optical parametric oscillators (OPOs); modulators and all-optically controlled, frequency up- and down-shifting NLO reflectors; and sensors in optical and microwave ranges of electromagnetic radiation [1–3].

Unparalleled properties of frequency mixing of *ordinary* contra-propagating waves were predicted in the beginning of the NLO era in the early 60s (see, e.g., [4] and references therein). NLO coupling of counter-propagating ordinary optical and acoustic waves was investigated in [5]. Extraordinary properties of photon-phonon coupling of two ordinary optical waves and one *backward* optical phonon wave were investigated in [6,7]. Parametric interaction of quasi-phase-matched counter-propagating ordinary optical waves in periodically poled nonlinear crystals was studied theoretically and experimentally in [8–12]. A review of four-wave mixing of ordinary contra-propagating waves in the context of optical phase conjugation is given in [13]. As concerns BEMWs, the current mainstream approach in engineering the MMs, which can support BEMWs, is to craft the MMs composed of plasmonic mesoatoms, which introduce negative μ and ε (negative-index MMs, NIMs) [1]. A broader class of MMs, which can ensure a whole set of the critically important NLO requirements—the coexistence and phase-matching of ordinary waves and BEMWs, which satisfy the energy conservation laws—was recently proposed in [14–18] based on the negative spatial dispersion and nanowaveguide operation regimes. Parametric interaction of ordinary and BEMWs was realized in the microwave transmission lines [19–21]. Miniaturization is intrinsic to MMs. Small NLO coupling volume dictates intense pulse excitation, which justifies the investigations described below. This Letter is to show fundamental differences in transient regimes in the BW and ordinary three-wave mixing (TWM) processes of the OPA and difference-frequency generation initiated by the pulse with a sharp forefront.

A remarkable difference in TWM, $\omega_1 = \omega_3 - \omega_2$, in the alternative cases of co- and contra-propagating waves at

frequencies ω_1 and ω_2 [Figs. 1(a) and 1(b)] is as follows. For co-propagating EMWs coupled in an ordinary loss-free material [Fig. 1(a)], a signal at ω_2 grows as $a_2(L) \sim \exp(gL)$. However, this dependence dramatically changes to $a_2(L) \sim 1/\cos(gL)$ in the case of Fig. 1(b) [22,23]. In the latter case, an ordinary wave at ω_2 propagates along the pump wave at ω_3 whereas the phase matched idler at ω_1 is a BEMW, which propagates in the opposite direction. Here, a_2 is the amplitude of the transmitted signal wave, L is the thickness of the NLO slab, and g is a factor proportional to NLO susceptibility and to amplitude a_3 of the pump wave at ω_3. In the latter case, the transmittance T_2 at ω_2 (OPA) experiences extraordinary enhancement as $gL \to \pi/2$. This value will be referred to as the critical value. The output idler at ω_1 contra-propagating in the *reflection* direction experiences a similar huge intensity-resonant enhancement. Such a "geometrical" resonance dependence of the TWM output on L (or on g) occurs due to the *internal distributed NLO feedback*, which is intrinsic to the contra-propagating setting. The outlined resonance dependence resembles resonance property of a cavity composed of two mirrors as the cavity length L or wave vector k_q approach resonance values. The latter occurs as two coherent contra-propagating waves meet each other to interfere destructively on the mirrors. Oscillation resonances are known to cause transient processes under pulsed excitation, which is the behavior intrinsic to any oscillator.

This Letter is to demonstrate unparalleled transient processes in the BW OPA and in the NLO reflectivity in the vicinity of the resonance intensities of the pump (control) field at ω_3. Such transients are *extraordinary* because they are not inherent to the TWM of co-propagating waves in ordinary materials. The outlined *frequency-shifting NLO reflectivity* also has no analog in the case of ordinary co-propagating TWM settings.

Consider interaction of three electromagnetic waves $E_j(z,t) = A_j(z,t)\exp\{i(\omega_j t - k_j z)\}$ $(j = 1, 2, 3)$ in a medium slab of length L with quadratic nonlinearity $\chi^{(2)}$. Wave vectors of all waves are codirected along the axis z. The relations $\omega_3 = \omega_1 + \omega_2$, $k_3 = k_1 + k_2$, and $(A_3 > A_1, A_2)$ are assumed to have been met. After introducing amplitudes $e_j = \sqrt{|\varepsilon_j|/k_j}A_j$, $a_j = e_j/e_{30}$, coupling parameters $æ = \sqrt{k_1 k_2/|\varepsilon_1\varepsilon_2|}4\pi\chi^{(2)}_{\text{eff}}$ and $g = æA_{30}$, where ε_1 and ε_2 are dielectric permittivity of the medium at the corresponding frequencies, $A_{j0} = A_j(z = 0)$, equations for electric components of waves in the approximation of slowly varying amplitudes can be written as follows:

$$\begin{cases} \partial a_1/\partial z + (1/v_1)\partial a_1/\partial t = -s_1[iga_3 a_2^* + (\alpha_1/2)a_1], \\ \partial a_2/\partial z + (1/v_2)\partial a_2/\partial t = -iga_3 a_1^* - (\alpha_2/2)a_2, \\ \partial a_3/\partial z + (1/v_3)\partial a_3/\partial \tau = -iga_1 a_2 - (\alpha_3/2)a_3. \end{cases} \quad (1)$$

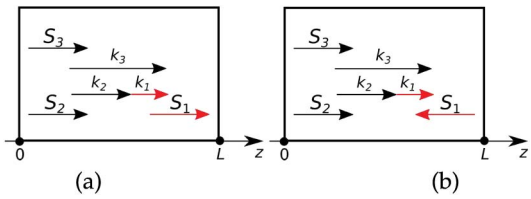

Fig. 1. Two alternative coupling options are (a) co-propagating waves and (b) contra-propagating signal and BW idler waves. Here, $\vec{k}_j$ are wave vectors and $\vec{S}_j$ are Poynting vectors.

Here, α_j are absorption indices and v_j are group velocities at the corresponding frequencies. For an ordinary wave at ω_1 [Fig. 1(a)], $v_1 > 0$, $s_1 = 1$. For BW at ω_1 [Fig. 1(b)], $v_1 < 0$, $s_1 = -1$. Quantities $|a_j|^2$ are proportional to the time dependent photon fluxes; g^{-1} is a characteristic slab length required for significant NLO energy transfer from the pump field A_3 to the signal at ω_2 and to the idler at ω_1. In the case of Fig. 1(a), the boundary conditions are defined as $a_{10} = 0$, $a_{20} = u$. In the case of Fig. 1(b), they change for $a_{1L} = 0$ and $a_{20} = u$, here $u \ll a_{30}$. It is readily seen, e.g., for the ultimate case of the continuous wave (CW) regime and $\alpha_j = 0$, that the indicated changes give rise to the fundamental transformation of the solution to the coupled Eq. (1) and to the appearance of the outlined geometrical resonance instead of exponential dependence [22].

We introduce the transmission (OPA) factor $T_2 = |a_{2L}(t)/a_{20}|^2$ and the NLO reflectivity factor $R_1 = |a_{10}(t)/a_{20}|^2$. Basically, two different regimes are possible. In the first one, the input pump A_{30} is a semi-infinite rectangular pulse and the input signal is a CW ($A_{20} = \text{const}$). In the opposite case, the pump is a CW and A_{20} is a semi-infinite rectangular pulse. First, consider the case of $v_3 = v_2 = -v_1 = v$. The shape of a semi-infinite pulse with a sharp front edge traveling with group velocity v along the axis z is given by function $F(t) = \{1 - \tanh[(z/v - t)/t_f]\}/2$, where parameter t_f determines its edge steepness. In the following numerical simulation, it is taken equal to $t_f = 0.05\Delta t$, where $\Delta t = L/v_3$ is a travel time of the fundamental pulse front edge through the slab. In the first case, $a_{30}(t) = a_{30}F(t)$, $a_{20} = \text{const}$. In the second case, $a_{20}(t) = a_{20}F(t)$, $a_{30} = \text{const}$. Here, a_{j0} is a maximum pulse amplitude magnitude at the slab entrance. The solution to Eq. (1) was obtained through numerical simulations.

Figure 2(a), the solid line, depicts the output signal at the slab exit ($z = L$) for the case of co-propagating ordinary waves, and the dashed line is for the case of a BW setting. It is seen that any changes in the output signal occur only after the travel period, both in the ordinary and BW regimes. For the case of the pulsed input pump and CW input signal, the output signal experiences amplification when the forefront of the pump pulse reaches the exit. For the co-propagating settings, the shape of the signal pulse almost follows the shape of the

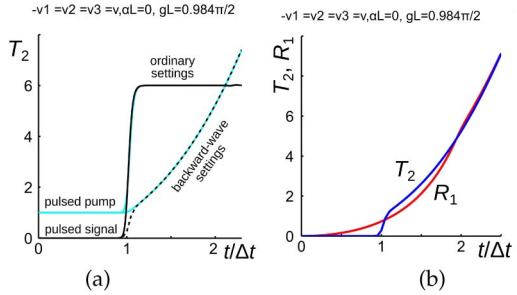

Fig. 2. (a) Difference in the transient processes under ordinary (the solid lines) and BW (the dashed lines) settings. $T_2(t)$ is the transmission (OPA) of the codirected seeding signal at the forefront area of the output signal pulse. (b) Difference in the transient processes in $T_2(t)$ and in nonlinear-optical reflectivity $R_1(t)$ (contra-propagating generated idler) for the case of the pulsed input signal and CW pump. (a) and (b): $-v_1 = v_2 = v_3 = v$, $\alpha_j = 0$, $gL = 0.984\pi/2$.

pump pulse. However, in the BW setting, the pulse shape changes dramatically in the vicinity of the resonance intensity of the pump wave, which corresponds to $gL = \pi/2$. The signal growth occurs slower; the output signal maximum is greater and is reached with significant delay. Figure 2(b) compares the transmitted signal at $z = L$ and the idler at $z = 0$ traveling in the reflection direction for the case of the pulsed input signal and the CW pump. It takes a travel time of Δt for the signal pulse to appear at $z = L$, whereas the idler is generated immediately after the pulse enters the slab. Hence, unlike the transmittance, the transients in the reflectivity are the same for the pulsed signal and pulsed pump modes. Figures 2(a) and 2(b) show that differences in OPA for the cases of the pulsed signal and the pulsed pump disappear after a period of time of about Δt, whereas the reflectivity and OPA develop in a similar way after a period of time of about $2\Delta t$.

Figure 3 depicts a more extended period of time. It demonstrates the rise time and the maximum OPA increase approaching the resonance strength of the pump field. It also demonstrates the fundamental difference between the rise periods and the eight-order difference in maxima achieved in the ordinary and BW TWM. It appears that calculated data can be approximated by the exponential dependence $T_2(t) = A(1 - \exp[-(t - \Delta t)/\tau])^2$ (the solid lines), where the rise time τ grows approximately as $1/\cos(gL)$ in the vicinity of the intensity resonance. For example, at $gL = 0.996\pi/2$, the fitting values are $A = 2.99 \cdot 10^4$, $\tau = 109.9\Delta t$. The short initial period (Fig. 2) is not resolved here. As outlined above, the transient processes in the OPA and in the NLO reflectivity are similar through the given time period.

Distributed NLO feedback gives rise to significant enhancement of the OPA and to depletion of the fundamental wave at $gL > \pi/2$. The latter leads to the stationary regime and to the decrease of the transient period (Fig. 4). As seen from Fig. 4(b), the delay of the output signal maximum relative to the pump maximum may reach impressive values on the order of hundreds of travel periods Δt. Maximum delay is reached at $gL = \pi/2$.

Absorption causes change in the delay time. For the case of the CW and neglected depletion of the pump, parameter g must be replaced by $g_{\text{eff}} = \sqrt{g^2 - (\alpha_1 + \alpha_2)^2/16}$ [23]. Hence, losses shift the maximum delay to $gL > \pi/2$ as seen in Figs. 5 and 6(a).

The transient period increases with the decrease of the group velocities (in the slow light regimes) as shown in Fig. 6(b).

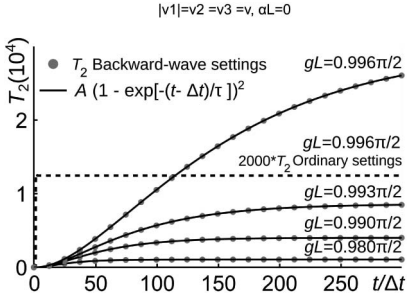

Fig. 3. Dependence of the transient OPA on the intensity of the pump field. The dashed line shows the TWM of co-propagating waves. Points correspond to ordinary signal and contra-propagating idler. The solid lines depict approximation of the transient OPA by the function $T_2(t) = A\{1 - \exp[-(t - \Delta t)/\tau]\}^2$. $-v_1 = v_2 = v_3 = v$, $\alpha_j = 0$.

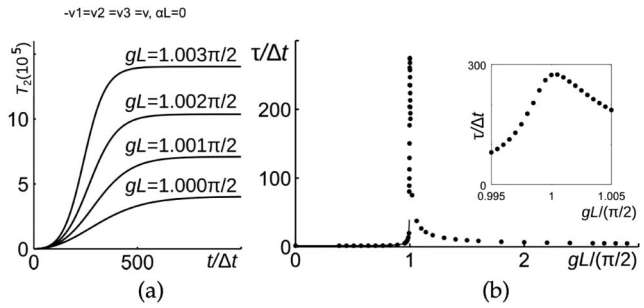

Fig. 4. (a) Shape of the signal forefront in transparent material at pump intensities above the critical input value $gL = \pi/2$. (b) Dependence of the transient period τ on the maximum intensity of the pump field. $-v_1 = v_2 = v_3 = v$, $\alpha_j = 0$.

Figures 7(a) and 7(b) depict dependence of the transient processes at the forefront of the output signal on the dispersion of group velocities. Figure 7(a) shows that the forefront of the output signal becomes steeper if it outruns the pump pulse. Figure 7(b) demonstrates that the pulse forefront also becomes steeper with an increase of the group velocity for the idler.

In the conclusion, we report extraordinary transient processes in optical parametric amplification and in the frequency-shifting NLO reflectivity. They originate from the TWM where one of the coupled waves travels against others. An example is investigated where the signal and the pump are ordinary co-propagating waves and the idler is the contra-propagating BW. Phase-matching is assumed achieved, i.e., all waves travel with the same phase velocities. The reference is given to the works showing how such a requirement can be satisfied. The energy flux (the group velocity) and the phase velocity are counter-directed in the BW. In this case, the phase-matching dictates energy flux in the BW (here, in the idler) to be directed against those in the pump and signal, i.e., in the reflection direction. Such coupling geometry gives rise to greatly enhanced coherent energy transfer from the pump to the signal and to the contra-propagating idler. We show that the enhanced coupling causes the transient processes in the TWM that have no analogs in the case of co-propagating couplings. Two options are investigated where the input pump is pulsed, whereas the input signal is a CW and vice versa. For the sake of explicitness, the ultimate case is investigated of a semi-infinite pulse with a sharp rectangular forefront entering a metamaterial slab. In both cases, the contra-propagating

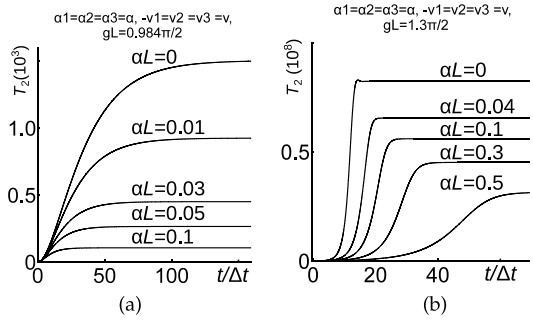

Fig. 5. Effect of absorption on the transient OPA for two different intensities of the pump field. $-v_1 = v_2 = v_3 = v$. $\alpha_1 = \alpha_2 = \alpha_3 = \alpha$. (a) $gL = 0.984\pi/2$. (b) $gL = 1.3\pi/2$.

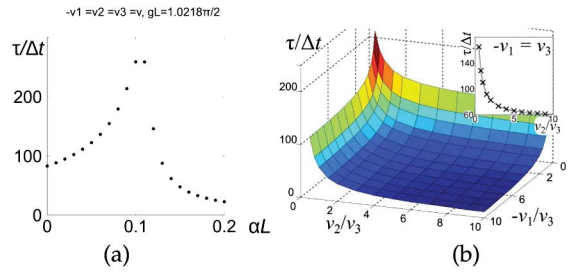

Fig. 6. (a) Effect of absorption on the transient period. $gL = 1.0218\pi/2$, $-\nu_1 = \nu_2 = \nu_3 = \nu$, $\alpha_1 = \alpha_2 = \alpha$, $\alpha_3 = 0$. (b) Dependence of duration of the transient period in the TWM on the group velocities of the coupled waves and on their dispersion. $\alpha_j = 0$, $gL = 0.996\pi/2$.

signal and idler, which exit the metaslab from the opposite sides, also appear as semi-infinite pulses, however, with the forefront significantly different from that of the input pulse. The results are contrasted by comparing the similar processes in the ordinary materials under standard settings where all coupled waves are co-propagating. The effects of changing the pump intensity, material absorption, and group velocity dispersion on the transient processes are investigated.

The major conclusions are as follows. There exists resonance value of the input pump intensity, which depends on the nonlinear susceptibility and on the thickness of the metaslab. Indicated extraordinary resonance provides giant enhancement in the three-wave coupling. Consequently, great enhancement occurs in optical parametric amplification of the signal and in the oppositely directed idler (in the frequency up- or down-shifted reflectivity). Such effect does not exist in the ordinary optical parametric amplification in the case of all codirected energy fluxes, where the indicated reflectivity does not exist at all. In the vicinity of the resonance intensity, extraordinary transient processes develop, which cause a change in the output-pulse shapes and a significant delay of their maximums. The latter is not the case under a co-propagating setting. The closer the pump intensity approaches the resonance value, the longer the transient period becomes. The delay in the output-pulse maximums relative to the input ones may occur up to several hundred times longer than the travel time of the fundamental pulse through the metaslab. A difference between the case of the input pulse pump and the case of the input pulse signal disappears after the time period of about the travel time for the fundamental pulse. The reflected pulse

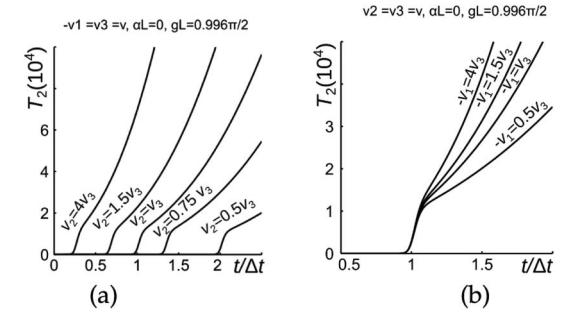

Fig. 7. Dependence of the transient TWM on the forefront of the output pulses on dispersion of group velocities of the coupled waves. $gL = 0.996\pi/2$, $\alpha_j = 0$. (a) $-\nu_1 = \nu_3$. (b) $\nu_2 = \nu_3$.

begins to develop immediately after the pump or the seeding pulse edges enter the slab, whereas the pulse in the amplified signal begins to form with the delay of about the travel time. The depletion of the pump at the input intensities above the resonance value causes a decrease in the rise time, which, therefore, has a maximum as a function of the input pulse intensity. Losses cause the shift of the maximum delay time to higher input pump intensities. The dispersion in the modules of the group velocities causes changes in the transient processes as well, which significantly depend on the particular difference between the group velocities of the coupled pulses.

The outlined coupling scheme and the revealed unparalleled properties must be accounted for at creation of advanced all-optically controlled optical amplifiers, filters, modulators, reflectors, and sensors implementing BEMWs. Similar processes are anticipated for the TWM of the ordinary contrapropagating waves achievable in crystals through quasi-phase-matching [8–12] and for the optical phase conjugation [13].

Funding. Army Research Office (ARO) (W911NF-14-1-0619); Ministry of Education and Science of the Russian Federation (214/71, 3.1749.2014/K); Russian Foundation for Basic Research (RFBR) (14-02-00219-a); Government of Krasnoyarsk Territory (16-42-240410p_a).

REFERENCES

1. W. Cai and V. Shalaev, *Optical Metamaterials, Fundamentals and Applications* (Springer-Verlag, 2010).
2. A. K. Popov and V. M. Shalaev, Proc. SPIE **8093**, 809306 (2011).
3. A. K. Popov, *Nonlinear, Tunable and Active Metamaterials*, I. V. Shadrivov, M. Lapine, and Y. S. Kivshar, eds. (Springer, 2015), Chap. 10, pp. 193–213.
4. S. E. Harris, Appl. Phys. Lett. **9**, 114 (1966).
5. D. L. Bobroff, J. Appl. Phys. **36**, 1760 (1965).
6. M. I. Shalaev, V. V. Slabko, S. A. Myslivets, and A. K. Popov, Opt. Lett. **36**, 3861 (2011).
7. A. K. Popov, M. I. Shalaev, S. A. Myslivets, V. V. Slabko, and I. S. Nefedov, Appl. Phys. A **115**, 523 (2014).
8. Y. J. Ding and J. B. Khurgin, IEEE J. Quantum Electron. **32**, 1574 (1996).
9. Y. J. Ding and J. B. Khurgin, Opt. Lett. **21**, 1445 (1996).
10. C. Conti and G. Assanto, Opt. Lett. **24**, 1139 (1999).
11. C. Canalias and V. Pasiskevicius, Nat. Photonics **1**, 459 (2007).
12. J. B. Khurgin, Nat. Photonics **1**, 446 (2007).
13. B. Y. Zel'dovich, N. F. Pilipetsky, and V. V. Shkunov, *Principles of Phase Conjugation*, Springer Series in Optical Sciences (Springer-Verlag, 1985), Vol. **42**, Chap. 6.
14. A. K. Popov, M. I. Shalaev, S. A. Myslivets, V. V. Slabko, and I. S. Nefedov, Appl. Phys. A **109**, 835 (2012).
15. A. K. Popov, I. S. Nefedov, S. A. Myslivets, M. I. Shalaev, and V. V. Slabko, Proc. SPIE **8725**, 87252E (2013).
16. A. K. Popov, V. V. Slabko, M. I. Shalaev, I. S. Nefedov, and S. A. Myslivets, Solid State Phenom. **213**, 222 (2014).
17. A. K. Popov, I. S. Nefedov, and S. A. Myslivets, "Phase matched backward-wave second harmonic generation in a hyperbolic carbon nanoforest," arXiv:1602.02497 (February 8, 2016).
18. C. Duncan, L. Perrel, S. Palomba, M. Lapine, B. T. Kuhlmey, and C. M. de Sterke, Sci. Rep. **5**, 08983 (2015).
19. K. I. Volyak and A. S. Gorshkov, Radioteknika *i* Elektronika **18**, 2075 (1973), in Russian.
20. A. B. Kozyrev, H. Kim, and D. W. van der Weide, Appl. Phys. Lett. **88**, 264101 (2006).
21. A. Rose, D. Huang, and D. R. Smith, Phys. Rev. Lett. **107**, 063902 (2011).
22. A. Yariv, *Quantum Electronics*, 3rd ed. (Wiley, 1988), p. 466.
23. A. K. Popov and V. M. Shalaev, Appl. Phys. B **84**, 131 (2006).